ADVANCING EARTH AND SPACE SCIENCES

JGR Oceans

RESEARCH ARTICLE

10.1029/2025JC023856

Key Points:

- Significant warming of Circumpolar Deep Water (CDW) off West Antarctica during 1990s–2010s, intensifying after 2010
- Strengthening Ross Gyre circulation during 2010s
- CDW warming off West Antarctica driven by Ross Gyre strengthening and cross-Antarctic Circumpolar Current heat transfer

Supporting Information:

Supporting Information may be found in the online version of this article.

Correspondence to:

B. Y. Damini,
brendon.oceano@furg.br

Citation:

Damini, B. Y., Dotto, T. S., Heywood, K. J., Naveira Garabato, A. C., Hall, R. A., Mata, M. M., & Kerr, R. (2026). Post-1990s warming of circumpolar deep water off West Antarctica and its drivers. *Journal of Geophysical Research: Oceans*, *131*, e2025JC023856. https://doi.org/10.1029/2025JC023856

Received 1 DEC 2025
Accepted 2 JUL 2026

Author Contributions:

Conceptualization: Brendon Y. Damini, Tiago S. Dotto, Karen J. Heywood, Alberto C. Naveira Garabato, Rob A. Hall, Mauricio M. Mata, Rodrigo Kerr
Formal analysis: Brendon Y. Damini
Investigation: Brendon Y. Damini
Methodology: Brendon Y. Damini, Tiago S. Dotto, Karen J. Heywood, Alberto C. Naveira Garabato, Rob A. Hall, Mauricio M. Mata, Rodrigo Kerr
Software: Brendon Y. Damini
Supervision: Tiago S. Dotto, Karen J. Heywood, Alberto C. Naveira Garabato, Rob A. Hall, Mauricio M. Mata, Rodrigo Kerr

Post-1990s Warming of Circumpolar Deep Water Off West Antarctica and Its Drivers

Brendon Y. Damini[1,2], Tiago S. Dotto[3], Karen J. Heywood[4], Alberto C. Naveira Garabato[5], Rob A. Hall[4,6], Mauricio M. Mata[1,2], and Rodrigo Kerr[1,2]

[1]Laboratório de Estudos dos Oceanos e Clima – LEOC, Instituto de Oceanografia, Universidade Federal do Rio Grande – FURG, Rio Grande, Brazil, [2]Programa de Pós-Graduação em Oceanologia, Instituto de Oceanografia, Universidade Federal do Rio Grande – FURG, Rio Grande, Brazil, [3]National Oceanography Centre, Southampton, UK, [4]Centre for Ocean and Atmospheric Sciences, School of Environmental Sciences, University of East Anglia, Norwich, UK, [5]Ocean and Earth Science, University of Southampton, Southampton, UK, [6]Scottish Association for Marine Science, Oban, UK

Abstract Ice loss off East Antarctica has been linked to the warming of Circumpolar Deep Water (CDW) associated with a poleward shift of the southern boundary of the Antarctic Circumpolar Current (ACC). In West Antarctica, where the fastest ice-shelf melting occurs, it has been proposed that off-shelf CDW warming could be additionally driven by enhanced lateral heat transport by a strengthened Ross Gyre and increased isopycnal heat transfer across the ACC. Although previous studies have proposed links between Ross Gyre variability, cross-ACC exchange, and off-shelf CDW warming around West Antarctica, their relative contributions have not yet been quantified. Here, we document an interdecadal (1990s–2010s) warming of off-shelf CDW around West Antarctica driven by two processes: (a) ~90% results from enhanced lateral heat transport along isopycnals at the ACC's southern boundary, linked to an intensification of the Ross Gyre and cross-ACC isopycnal heat transfer; and (b) ~10% arises from a poleward expansion of the ACC's hydrographic structure, analogous to that observed off East Antarctica. Both sets of processes were concurrent with a strengthening and poleward shift of westerly winds over the Southern Ocean, suggesting a causal link. As climate projections indicate that such wind trends will continue through the 21st century, the ongoing off-shelf CDW warming may also persist in future, bolstering the shelf break source of oceanic heat supply to the West Antarctic Ice Sheet.

Plain Language Summary In West Antarctica, relatively warm water, known as Circumpolar Deep Water (CDW), is stored below the surface. When this warm water moves onto the continental shelf, it can melt ice shelves and contribute to sea-level rise. Since the 1990s, off-shelf CDW has warmed substantially. Previous studies suggested that this warming could be linked to two mechanisms: changes in the strength of the Ross Gyre, a large regional ocean circulation, and processes associated with the Antarctic Circumpolar Current (ACC). These include increased exchanges of water across the ACC and a poleward shift of its southern boundary, north of the continental shelf. Here, we show that CDW warmed significantly over the last three decades, and that about 90% of this warming was driven by an intensification of the Ross Gyre and enhanced poleward transfer of warm water across the ACC. Both processes were associated with stronger, poleward-shifted westerly winds over the Southern Ocean, consistent with a causal link. As climate projections suggest, these wind trends will continue through the 21st century, CDW warming may also persist. If so, it would further increase the heat reservoir north of the continental shelf that supplies oceanic heat to West Antarctic ice shelves, threatening their stability.

1. Introduction

The Antarctic Ice Sheet has been losing mass at an accelerated rate since at least the 1970s and now accounts for approximately 15% of global sea-level rise (e.g., Frederikse et al., 2020). The most rapid loss and disintegration of ice shelves in recent decades have been observed along the West Antarctic margins (e.g., Rignot et al., 2019). This retreat has primarily been driven by enhanced intrusions of relatively warm Circumpolar Deep Water (CDW) via submarine glacial troughs (e.g., Dutrieux et al., 2014). In the Antarctic subpolar zone, off-shelf CDW circulates within the intermediate layers of the Antarctic Circumpolar Current (ACC), particularly near its southern edge, close to the Southern ACC Front (SACCF) and the Southern Boundary Front (e.g., Orsi et al., 1995).

Previous studies indicate that the CDW layer off-shelf has warmed over the past few decades (Sallée, 2018; Schmidtko et al., 2014). In East Antarctica (115°–150°E), this warming is mainly attributed to poleward

Visualization: Brendon Y. Damini
Writing – original draft: Brendon Y. Damini
Writing – review & editing: Brendon Y. Damini, Tiago S. Dotto, Karen J. Heywood, Alberto C. Naveira Garabato, Rob A. Hall, Mauricio M. Mata, Rodrigo Kerr

displacement of ACC fronts and their hydrographic structure driven by intensifying westerly winds (Herraiz-Borreguero & Naveira Garabato, 2022; Yamazaki et al., 2021). Additionally, enhanced isopycnal transfer of CDW across the ACC, facilitated by both Ekman processes and eddy activity, may further contribute to this warming (Herraiz-Borreguero & Naveira Garabato, 2022; Yamazaki et al., 2021, 2023; Zu et al., 2022). This off-shelf CDW warming has enhanced oceanic heat delivery to ice shelves, likely contributing to the recent acceleration of ice-mass loss in East Antarctica (Herraiz-Borreguero & Naveira Garabato, 2022).

In West Antarctica, the supply of CDW to the shelf break region has been proposed to occur primarily via isopycnal heat transport. Such transport may be affected by: (a) lateral heat transfer within the SACCF, associated with the Ross Gyre's eastward extension; this has been illustrated by modeling studies, which indicate that expansion of the gyre's eastern limb under increased cyclonic wind stress curl can enhance poleward heat transport toward the West Antarctic shelf break (Castagno et al., 2017; Gómez-Valdivia et al., 2023; Nakayama et al., 2018; Prend et al., 2024); and (b) cross-ACC isopycnal exchanges, driven by mesoscale eddy activity (e.g., Marshall & Speer, 2012; Thompson & Naveira Garabato, 2014). Both (a) and (b) are expected to respond dynamically to the documented ongoing poleward intensification of the westerly winds over the Southern Ocean, which would result in a strengthening of both transport processes (e.g., Prend et al., 2024; Marshall & Speer, 2012).

Although previous studies have discussed the potential links between these processes and changes in the thermohaline properties of CDW off West Antarctica (e.g., Marshall & Speer, 2012; Prend et al., 2024), the processes' relative contributions have not been quantified with observations, and neither has that from meridional displacements of ACC fronts. Here, we investigate interdecadal changes (1990s–2010s) in CDW properties in both the off-shelf and continental shelf regions around West Antarctica (120°–70°W; 67.5°–74°S) using hydrographic observations and a high-resolution ocean reanalysis. We identify a warming of the CDW off West Antarctica in both data sets and quantitatively elucidate its drivers. Our analysis indicates that the observed off-shelf CDW warming has been mainly driven by a lateral heat transfer linked to a stronger Ross Gyre and to enhanced cross-ACC isopycnal heat transport. A poleward expansion of the southern edge of the ACC's hydrographic structure made a secondary contribution to the warming. All drivers are associated with a poleward shift and intensification of the westerly winds. Despite this overall off-shelf warming, the continental shelf exhibits spatial heterogeneity in its hydrographic response, reflecting the influence of regional wind patterns at the shelf break (e.g., Huguenin et al., 2024) and thermodynamic processes (i.e., vertical convection driven by surface heat loss) on the highly variable shelf (Oelerich et al., 2022).

2. Materials and Methods

2.1. Hydrographic and GLORYS12v1 Data Set

The data set used here encompasses hydrographic measurements of temperature and salinity from: World Ocean Database 2023 (https://www.ncei.noaa.gov/products/world-ocean-database); Thwaites-Amundsen Regional Survey and Network (TARSAN; https://www.bodc.ac.uk/data/bodc_database/nodb/project/54319/); Argo (https://argo.ucsd.edu); the CLIVAR and Carbon Hydrographic Data Office (https://cchdo.ucsd.edu/); and the Marine Mammals Exploring the Ocean Pole to Pole consortium (MEOP; https://www.meop.net/, spanning 1990–2020; Figure S1 in Supporting Information S1). The hydrographic measurements of temperature and salinity were collected by electronic conductivity-temperature-depth (CTD) sensors with temperature and salinity accuracies of 0.001°C and 0.002, respectively (Mishonov et al., 2024). For Argo profiles, accuracies are 0.002°C and 0.0035 (Cowley et al., 2021; Riser et al., 2015), while the MEOP data set, predominantly concentrated along the continental shelf, reports accuracies of 0.02°C and 0.03 for temperature and salinity, respectively (Roquet et al., 2011; Siegelman et al., 2019). Importantly, the temperature and salinity changes observed along the continental shelf exceed the MEOP data set's accuracy thresholds (0.02°C for temperature and 0.03 for salinity), supporting the robustness of our findings. For each hydrographic station, spurious hydrographic data greater than two standard deviations from the mean value of each profile were removed.

Hydrographic properties spanning 120°–70°W and 67.5°–74°S were grouped by decade (1990s, 2000s, and 2010s) and interpolated onto a 0.25° grid using radial basis function interpolation with a linear weighting. The radial basis function interpolation method was chosen for its flexibility in adapting to the spatial structure of the data, making it particularly effective for irregular or sparse data sets (Damini et al., 2025; Yamazaki et al., 2021). Since we have spatial data gaps, we decided to apply an interpolation method to calculate the difference between the decades and the time-average over the entire period. Additionally, we opted to mask areas with no data points within a 50 km radius (∼2 times the grid spacing), ensuring greater robustness for our analyses.

We assessed the ability of GLobal Ocean Reanalysis and Simulation (GLORYS) to reproduce thermohaline variability by examining whether similar patterns are evident in hydrographic data for the same period and the same region. For this, we again analyzed hydrographic properties (i.e., temperature and salinity) grouped by decades (the 1990s, 2000s, and 2010s). GLORYS is a global eddy-resolving physical ocean and sea ice reanalysis with 1/12° horizontal resolution and 50 standard vertical levels. It covers the period from 1993 to the present, is based on the Nucleus for European Modeling of the Ocean platform (NEMO), and is atmospherically forced with ERA-Interim (https://www.ecmwf.int/en/forecasts/dataset/ecmwf-reanalysis-interim/). Quality assessments have shown that GLORYS effectively captures the main interannual climate variability signals for the ocean and sea ice (Jean-Michel et al., 2021).

2.2. CDW Layer Definition

We calculated conservative temperature—Θ, °C, and absolute salinity—S_A, g kg^{-1}, using the International Thermodynamic Equation of Seawater – 2010 (TEOS-10) (McDougall & Barker, 2011) from hydrographic measurements and GLORYS. The CDW layer was defined as the maximum Θ below 300 m, thereby excluding the influence of surface processes such as buoyancy forcing. This criterion identifies the CDW core (Figures S2 and S3 in Supporting Information S1; e.g., Schmidtko et al., 2014), which occupies intermediate layers along the SACCF around West Antarctica (e.g., Orsi et al., 1995). In the study region, the CDW layer typically occurs within a neutral density (γ^n) range of $\gamma^n \approx 27.93$–28.03 kg m^{-3} (Yamazaki et al., 2024). Similar results are obtained when temperature variability is evaluated directly along these neutral density surfaces (Figure S4 in Supporting Information S1).

2.3. SACCF Definition

The southern edge of the ACC can be identified in hydrographic sections across the Southern Ocean as the zone where CDW reaches its southernmost extent and upwells (Orsi et al., 1995). This boundary is commonly described as comprising two distinct hydrographic fronts: the SACCF and the Southern Boundary (Chapman et al., 2020; Orsi et al., 1995). However, as noted by Orsi et al. (1995), these two fronts are often separated by only a few tens of kilometers and tend to migrate meridionally in a coherent fashion. Accordingly, for this study, we treat the SACCF-Southern Boundary system as a single, unified feature and trace it in terms of the SACCF.

Historically, ACC fronts in this region have been defined based on hydrographic water mass properties (e.g., Orsi et al., 1995). In this study, we follow this hydrographic definition and identify the SACCF as the location where the 1.8°C isotherm within CDW intersects 500 m depth, using both interpolated hydrographic observations and GLORYS12v1 output for each decade (see Section 2.1). Additionally, because ACC fronts are associated with strong geostrophic flows, their positions are expected to correspond to gradients in Absolute Dynamic Topography (ADT), representing sea surface height relative to the geoid (Kim & Orsi, 2014; Sokolov & Rintoul, 2009a, 2009b). To evaluate the consistency of our SACCF defined from the 1.8°C isotherm with satellite observations, we additionally analyzed summer-mean (January–March; to minimize the noise in SACCF definition due to sea ice cover) ADT fields provided by Copernicus with a spatial resolution of 0.25° × 0.25° spanning 1993 to 2020.

Our analysis revealed a close match between the hydrographic, GLORYS output definition and the ADT = −1.10 m contour (Figure S5a in Supporting Information S1). In addition, we found a consistent close match between the SACCF positions derived from our hydrographic, GLORYS, and satellite altimetry definitions and the data set of ACC positions from Orsi et al. (1995). Furthermore, the time-averaged (1990–2020) SACCF positions derived from GLORYS output show a significant correlation (r) with p-value <0.05 with those from hydrographic measurements, satellite altimetry and data set of ACC positions from Orsi et al. (1995) ($r = 0.94$, $r = 0.96$ and $r = 0.70$, respectively; Figure S5a in Supporting Information S1), reaffirming the reliability of our findings.

To analyze the meridional displacement of the SACCF between the 1990s and 2010s, we first calculated the average SACCF position (latitude and longitude) for each decade. These data were then aligned onto a common longitude grid, enabling a direct comparison of latitudinal displacements. Additionally, to ensure that the interdecadal poleward SACCF displacement is robust against interannual variability, we performed a sensitivity analysis using sliding 10-year windows for both the historical (1993–2004) and modern (2009–2020) periods. The poleward shift remains statistically consistent across all temporal permutations (Table S1 in Supporting Information S1).

Because the SACCF definition used here is based on fixed values of isotherm and ADT, its position may be influenced by long-term thermodynamic changes of the CDW layer and long-term steric changes of the water column (Chapman et al., 2020). Previous studies using alternative dynamical diagnostics based on meridional gradients of ADT (Kim & Orsi, 2014) did not yield a unique and spatially continuous frontal position, likely due to strong frontal meandering and mesoscale variability (Figure S6 in Supporting Information S1; Chapman, 2014), resulting in a weak meridional ADT-gradient signature for the SACCF (Schiavon et al., 2025). Consequently, we retain the hydrographic definition to maintain consistency with recent literature (Herraiz-Borreguero & Naveira Garabato, 2022; Yamazaki et al., 2021), explicitly acknowledging its inherent inability to fully decouple kinematic frontal displacements from the thermodynamic changes of the CDW layer.

2.4. Calculation of Dynamic Height From Hydrographic Profiles

Following Yamazaki et al. (2021), the dynamic height (Φ) was calculated by vertically integrating specific volume from 300 dbar to 1,800 dbar for each point on the GLORYS grid north of the continental shelf (Figure S7a in Supporting Information S1). This range of Φ was chosen because values above 2,000 dbar accurately represent the position of the equivalent barotropic ACC fronts (e.g., Meijers et al., 2011), while temperatures above 300 dbar are more influenced by small-scale processes than by the frontal position (e.g., mixing processes in the mixed layer; Yamazaki et al., 2021).

2.5. Changes in Conservative Temperature of CDW Due To Meridional ACC Displacements

Here, the CDW layer changes are explained by two main mechanisms. To this end, we decompose the changes into two components to elucidate their underlying causes in geographical space. In Equation 1, $\Delta\Theta(x, y)$ represents the changes in Θ along the geostrophic contour of the equivalent barotropic ACC front, reflecting decadal changes in conservative temperature within the CDW layer. The first term on the right hand side, $\Delta\Theta_{\mathrm{front}}$ (hereafter referred to as the frontal shift; Equation 2), accounts for Θ changes associated with the meridional displacements of Φ, representing the Eulerian response to frontal displacements. In other words, this term considers the barotropic effect induced by the southern expansion of the southern edge of the ACC's hydrographic structure on temperature changes throughout the CDW layer. The second term, $\Delta\Theta'(x, y)$, is computed here as the residual of Equation 1. This term corresponds to the along-streamline changes, that is, the temperature change occurring along the geostrophic contour of the equivalent barotropic SACCF, driven by baroclinic processes, such as for example, eddy activity and lateral heat advection along isopycnals.

$$\Delta\Theta(x,y) = \Delta\Theta_{\mathrm{front}}(x,y) + \Delta\Theta'(x,y). \quad (1)$$

$\Delta\Theta(x, y)$ was quantified directly from GLORYS output, subtracting the 2010s time-average Θ in the CDW layer field from that of the 1990s, thus highlighting the interdecadal change in CDW properties. $\Delta\Theta_{\mathrm{front}}$ was calculated as follows:

$$\Delta\Theta_{\mathrm{front}}(x,y) = \Delta\Phi(x,y) \times \frac{\partial\Theta}{\partial\Phi}, \quad (2)$$

where $\Delta\Phi(x, y)$ was obtained by subtracting the 1990s time-average Φ field (see Calculation of Φ) from that of the 2010s (Figure S7b in Supporting Information S1). Additionally, we applied a low-pass spatial filter to the decadal climatologies of dynamic height of ~3 times the meridional grid spacing to attenuate spatial scales smaller than 50 km. This filtering removes eddy-like features or artifact residuals that are irrelevant to the frontal position. $\frac{\partial\Theta}{\partial\Phi}$ is determined by fitting a least-squares linear relationship between Θ of the CDW layer climatology and the climatological Φ (Figures S7c and S7d in Supporting Information S1). Sensitivity tests using alternative depth ranges of Φ (e.g., 400 dbar to 1,800 dbar and 300 to 1,500 dbar) showed similar results. The strong correlation between Φ and CDW temperature variability remained consistent across all definitions ($r = 0.97$, $p < 0.01$; Figure S7d in Supporting Information S1). This confirms that the analysis is not sensitive to the exact depth ranges selected. We highlighted that the above method for assessing the influence of the SACCF's poleward displacement on CDW warming cannot be applied in regions that encompass the continental slope and continental shelf, where circulation features such as the Antarctic Slope Current and the Amundsen Sea undercurrent may introduce strong non-equivalent barotropic structure.

2.6. Ancillary Data Sets

The summertime (January–March) monthly wind and sea level pressure (SLP) data sets were analyzed to investigate how climate-driven changes in atmospheric forcing may have influenced the CDW layer variability in both the continental shelf and off-shelf regions of Antarctica. These data sets were obtained from the ERA5 reanalysis (Hersbach et al., 2020), which features a horizontal resolution of 0.25° and is considered to provide one of the most accurate representations of climate conditions over Antarctica (Dong et al., 2020). Using summertime means of SLP, and zonal and meridional winds, we calculated decadal averages of their anomalies relative to the 1990–2020 climatology, as well as decadal changes of these anomalies (i.e., anomalies of the 2010s minus anomalies of the 1990s). This approach offers a first-order assessment of the prevailing atmospheric conditions around West Antarctica for each period. We also examined decadal anomalies of wind stress curl (calculated following Veny et al., 2024) relative to the 1990–2020 climatology. That analysis indicated the wind-driven upwelling of subsurface water masses, including CDW. In addition, we tracked the latitudinal position of the southern hemisphere maximum westerly jet following Goyal et al. (2021), which identifies the latitude of maximum summertime zonal wind speed between 30°S and 70°S and averages these peak latitudes across all longitudes for each decade.

3. Results and Discussion

3.1. Interdecadal Off-Shelf CDW Warming off West Antarctica

Hydrographic measurements off-shelf around the SACCF (defined by −1.10 m contour of ADT, and validated by hydrographic measurements using 1.8°C isotherm within the CDW layer intersects 500 m depth and the ACC frontal position from Orsi et al. (1995)) reveal a widespread significant CDW layer warming of ∼0.10 ± 0.05°C (Figure 1a); and salinification of ∼0.02 ± 0.01 g kg^{-1} (Figure 1b) between the 1990s and 2010s. For both properties, the reported uncertainty represents the standard deviation of the area-averaged values. These warmer and saltier signals generally align with the results reported by Zu et al. (2022), who documented increased temperature and salinity of CDW along East Antarctica from 2006 to 2020. This suggests a potentially circumpolar change of the CDW.

The sparseness of hydrographic observations, particularly before the Argo period, which began in the 2000s, hampers any evaluation of the dynamic links between off-shelf and continental shelf signals. Therefore, we used the high-resolution GLORYS reanalysis to explore the CDW variability in more detail. Here, we divided the series into conventional decades; that is, 1990s represent the period of 1993–2000, 2000s represent the period of 2001–2010, and 2010s represent the period of 2011–2020. A Hovmöller analysis over the off-shelf region (Figure 2) revealed that this choice highlights the interdecadal change in CDW properties, with warming and salinification becoming particularly pronounced after 2010. This timing mirrors the off-shelf CDW warming reported by Herraiz-Borreguero and Naveira Garabato (2022), and coincides with a transition toward a warmer continental shelf regime in areas of East Antarctica, where warm modified CDW became more widespread after ∼2010 (Ribeiro et al., 2023). Therefore, such interdecadal warming may increase the availability of heat that can potentially access the continental shelf through troughs (see discussion in Section 3.3).

GLORYS also shows a significantly warmer (∼0.1 ± 0.02°C) and saltier (∼0.02 ± 0.01 g kg^{-1}) off-shelf CDW layer around the SACCF (defined by 1.8°C at depths >500 m in the GLORYS reanalysis, and validated by hydrographic measurements, ADT, and the ACC frontal position from Orsi et al. (1995)) during the 2010s relative to the 1990s, in agreement with the sparse observations (Figures 1c and 1d). The decadal variations of conservative temperature in the off-shelf CDW layer between the 2010s and 2000s (∼0.06 ± 0.02°C) and between the 2000s and 1990s (∼0.03 ± 0.01°C) suggest a gradual and consistent off-shelf warming. Despite pronounced interannual variability (Figure 2), the long-term evolution of CDW temperature is well approximated by a linear trend from 1993 to 2020. In this sense, we found a significant off-shelf CDW warming at the SACCF of ∼0.05°C per decade over the full study period (Figure S8 in Supporting Information S1). This estimate, although slightly smaller, is qualitatively consistent with the warming trend of ∼0.1°C per decade reported by Schmidtko et al. (2014) for West Antarctica during 1975–2012. Moreover, our findings align with previous studies that

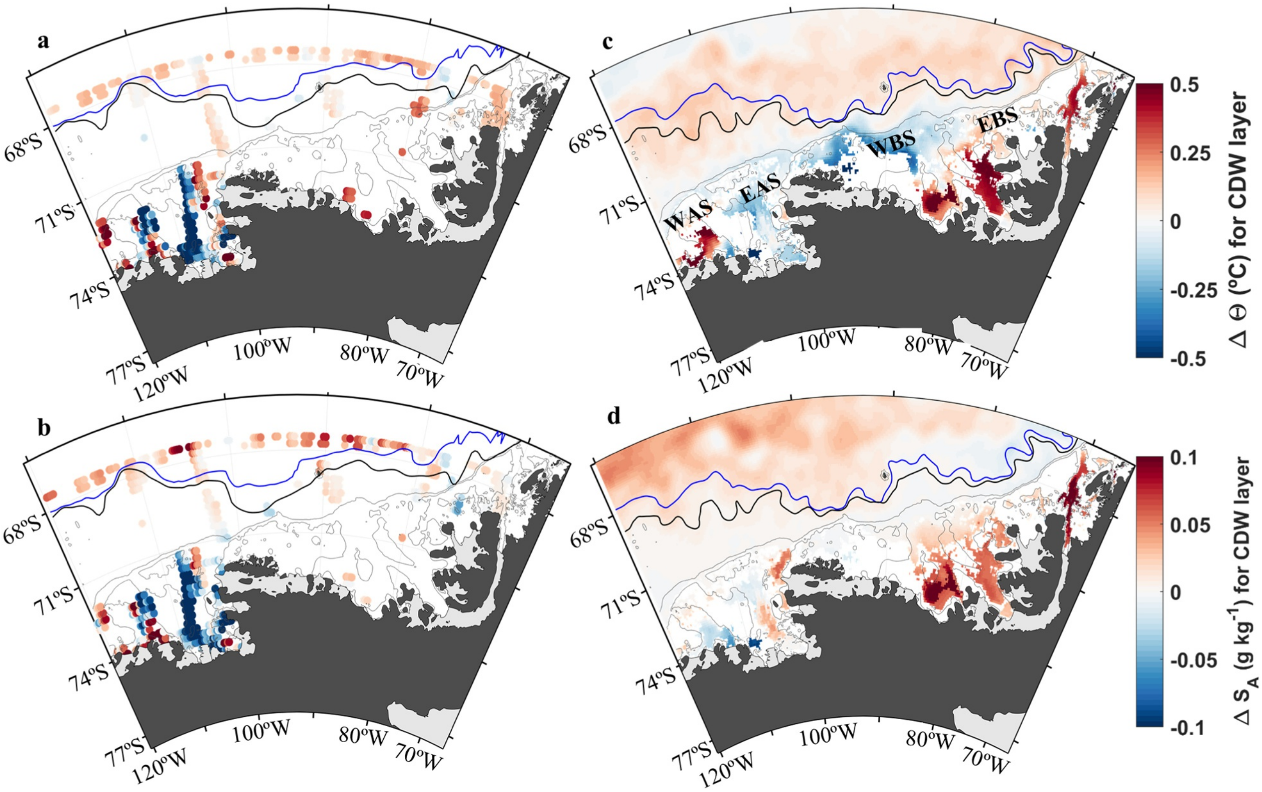

Figure 1. Decadal changes in the properties of the CDW layer, defined as the maximum Θ below 300 m. Difference between 2010s and 1990s in (a) Conservative Temperature (Θ, °C) and (b) Absolute Salinity (S_A, g kg^{-1}) from hydrographic measurements and (c, d) from GLORYS output. Blue and black lines indicate the mean positions of the Southern Antarctic Circumpolar Current Front during the 1990s and 2010s, respectively, based on satellite altimetry (a, b) and GLORYS output (c, d). Thin gray contours represent the 500 m and 1,500 m isobaths from the R–Topo2 data set (Schaffer et al., 2016). The labels WAS, EAS, WBS, EBS denote the Western Amundsen Sea, Eastern Amundsen Sea, Western Bellingshausen Sea, Eastern Bellingshausen Sea, respectively.

suggested a circumpolar warming of up to ~0.2°C per decade since the 1970s in waters below 200 m (e.g., Auger et al., 2021; Böning et al., 2008; Gille, 2002, 2008; Sallée, 2018). The CDW warming identified here may result from two distinct mechanisms, both of which may be enhanced by an intensification and poleward displacement of the westerly winds. Below, we will assess these candidate mechanisms in more detail.

3.2. Potential Mechanisms Driving Off-Shelf CDW Layer Warming

The first mechanism considers the ACC frontal displacement, which represents a poleward expansion of the southern edge of the ACC's hydrographic structure (Gille, 2002; Herraiz-Borreguero & Naveira Garabato, 2022; Meijers et al., 2011; Orsi et al., 1995; Yamazaki et al., 2021). Although previous studies suggested that the circumpolar-mean position of the ACC has remained broadly stable over recent decades (e.g., Gille, 2014), such averages may mask substantial regional variability. The ACC does not respond uniformly to atmospheric forcing across longitudes and cannot be treated as a single coherent dynamical feature (Kim & Orsi, 2014). Here, we provide evidence for a regional poleward displacement of the SACCF in the West Antarctic sector during the 2010s, supported by both GLORYS output (Figures 3a and 3b and Figures S5a and S10a in Supporting Information S1), hydrographic measurements, and satellite altimetry (Figures S5b and S5c in Supporting Information S1). This displacement is consistent with recent studies documenting regional migrations of ACC fronts (Herraiz-Borreguero & Naveira Garabato, 2022; Park et al., 2019; Yamazaki et al., 2021). The quantitative discrepancy between GLORYS and satellite altimetry may reflect the relatively coarse horizontal resolution of altimetry (0.25° × 0.25°), which cannot fully resolve mesoscale processes with horizontal scales of ~10 km (e.g., eddy–mean flow interactions; McKee et al., 2019) that influence decadal frontal variability. Furthermore, a Hovmöller analysis between 120°W and 70°W of the summer-averaged SACCF position based on the GLORYS output definition captures a clear long-term poleward displacement, with an average of 26.13 ± 17.29 km since

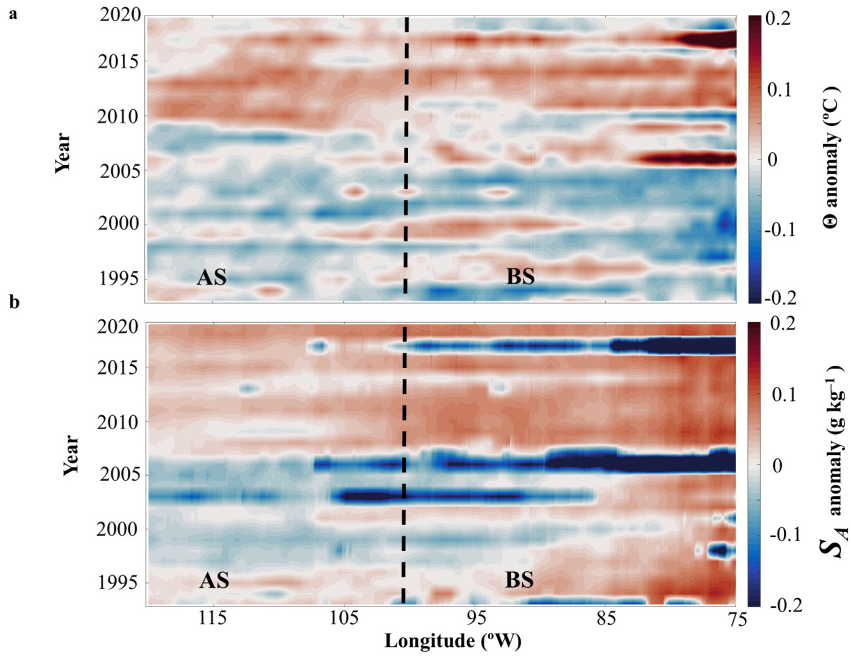

Figure 2. Evolution of CDW layer properties at the SACCF position. (a) Conservative Temperature (Θ, °C) anomalies relative to the 1993–2020 mean (b) Same as panel (a), but for Absolute Salinity (S_A, g kg^{-1}) anomalies.

2009–2010. It highlights high interannual variability in the SACCF position over the region (Figure 3). However, because the CDW layer also warmed significantly during the study period, we cannot exclude a thermodynamic contribution to the apparent displacement of the SACCF and therefore interpret this signal cautiously. In this sense, further studies using complementary dynamical diagnostics will be needed to better separate dynamical frontal migration from long-term ocean thermodynamic changes.

We analyzed the Southern Hemisphere maximum westerly winds' position and SLP to assess possible mechanisms that contribute to the poleward displacement of the SACCF. The decadal position of the Southern Hemisphere maximum westerly winds exhibited a poleward shift during the 2010s (Figures 3c and 3d and Figure S10b in Supporting Information S1). Concurrently, a significant decline in SLP anomaly around West Antarctica between the 1990s and the 2010s was observed (Figures 3c and 3d), which indicates a deepening and intensification of the Amundsen Sea Low—ASL (a persistent low-pressure system that strongly modulates wind fields in this region; Raphael et al., 2016; Turner et al., 2017). This deepening and intensification of the ASL during the 2010s is associated with a strengthening of westerly winds driven by an increased meridional SLP gradient between the mid-latitudes and the polar region (Clem & Fogt, 2015; Hosking et al., 2013; Raphael et al., 2016). As the ACC is primarily wind-driven, the position of its fronts is closely linked to the structure and variability of the wind field (e.g., Meredith, 2016). Hence, it is expected that the observed intensification and poleward migration of westerly winds in the 2010s may be the mechanism responsible for the observed southward expansion of ACC fronts around West Antarctica. This result aligns with previous studies showing that variability in the westerly winds can modulate ocean circulation and frontal positions around Antarctica (e.g., Herraiz-Borreguero & Naveira Garabato, 2022; Mizobata et al., 2025). In particular, Herraiz-Borreguero and Naveira Garabato (2022) showed that poleward displacement of SACCF by ∼100–200 km in East Antarctica was largely aligned with variability in the westerly winds.

Because surface forcing weakens below 300 m, the increase in off-shelf CDW heat content along the SACCF must arise from advective processes at intermediate depths. We suggest that this CDW warming results from a wind-driven circulation response that enhances both cross-ACC isopycnal exchange (e.g., Marshall & Speer, 2012; Yamazaki et al., 2023) and lateral isopycnal heat transport associated with a strengthening of the Ross Gyre (Gómez-Valdivia et al., 2023; Nakayama et al., 2018; Prend et al., 2024). Firstly, intensified westerly winds during the 2010s, indicated by the deepening and intensification of the ASL (Figure 3b), can enhance baroclinic instability along the ACC, potentially increasing mesoscale eddy activity (Zhang et al., 2021). This

10.1029/2025JC023856

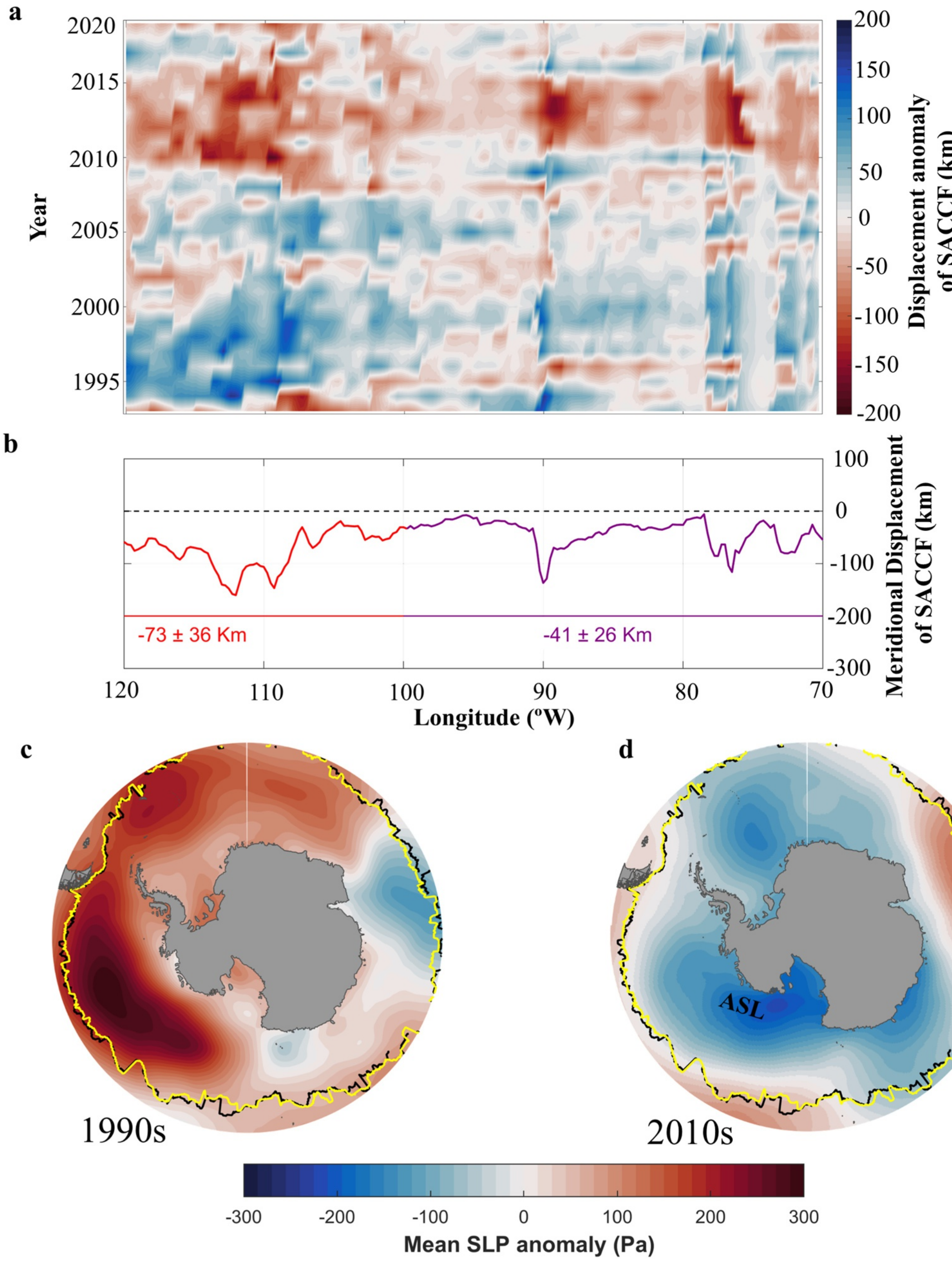

Figure 3. Decadal changes in the position of SACCF. (a) Hovmöller diagram of the displacement anomaly of SACCF (in km) relative to the period 1990–2020 based on GLORYS output. Positive values show the Southern Antarctic Circumpolar Current Front—SACCF displacement poleward, while negative values show the SACCF displacement equatorward; (b) Meridional displacement of the SACCF derived from GLORYS output. The Amundsen Sea region is highlighted in red and Bellingshausen Sea region in purple. Also indicated is each region's average meridional displacement (in km); (c) Sea level pressure (SLP, Pa) anomaly for the 1990s, relative to the period 1990–2020; (d) same as panel (c) but for the 2010s. The black (yellow) solid lines indicate the summertime Southern Hemisphere maximum westerly position averaged for the 1990s (2010s).

interpretation is consistent with the significant positive trend in eddy kinetic energy (9.7 ± 7.5 cm^2 s^{-2}) observed across the Pacific sector of the ACC (150°E−60°W) between 1993 and 2018 (Zhang et al., 2021). Enhanced eddy activity in this sector may facilitate cross-frontal exchange by advecting CDW poleward and diffusively redistributing heat along isopycnals through eddy stirring (e.g., Dufour et al., 2015; Ferrari & Nikurashin, 2010; Yamazaki et al., 2023). On the other hand, intensified westerlies strengthen the negative wind-stress curl over the

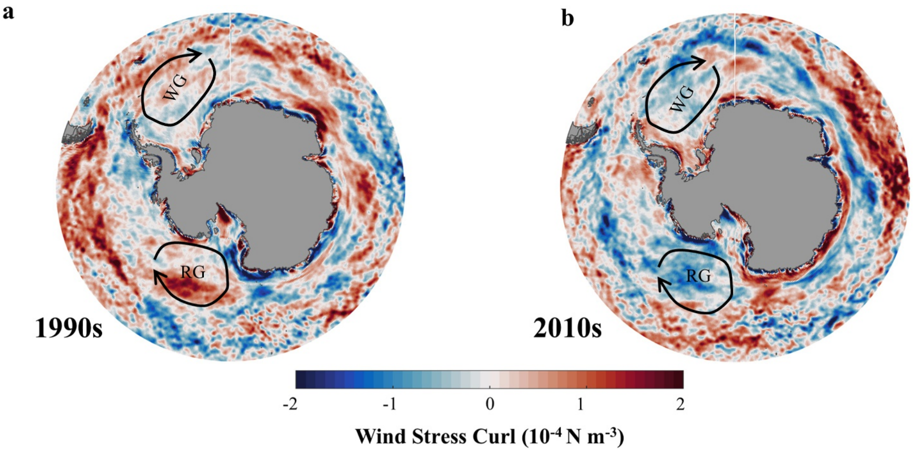

Figure 4. Decadal changes in the wind stress curl. (a) Wind stress curl (N m^{-3}) anomaly for the 1990s, relative to the period 1990–2020; (b) same as panel (a) but for the 2010s. Positive anomalies indicate reduced Ekman upwelling, whereas negative anomalies denote enhanced Ekman upwelling. Black arrows mark the approximate positions of the Ross Gyre (RG) and the Weddell Gyre (WG).

Ross Gyre region (Figure 4), consistent with enhanced cyclonic vorticity input to the ocean (Dotto et al., 2018). Through geostrophic adjustment, this forcing intensifies and expands the Ross Gyre circulation (Gómez-Valdivia et al., 2023; Nakayama et al., 2018; Prend et al., 2024). Changes in gyre strength are closely tied to shifts in the position and extent of its eastern limb, which acts as a conduit transporting CDW poleward toward the continental slope (e.g., Nakayama et al., 2018). An intensified gyre therefore increases southward heat transport along this boundary, enhancing the supply of CDW at intermediate depths that is subsequently advected laterally along isopycnals toward West Antarctica.

The relative contributions of these mechanisms to the observed off-shelf CDW warming along the SACCF were evaluated using a decomposition of isopycnal temperature changes. Our results indicate that frontal displacement contributes approximately 0.01°C (∼10%; Figure 5a), consistent with a modest increase in dynamic height of up to 0.1 m^2 s^{-2} (Figure S7b in Supporting Information S1). However, this contribution varies regionally, and in some locations frontal movement is associated with local cooling (Figures 1c and 5a), indicating that frontal displacement alone cannot explain the overall warming signal.

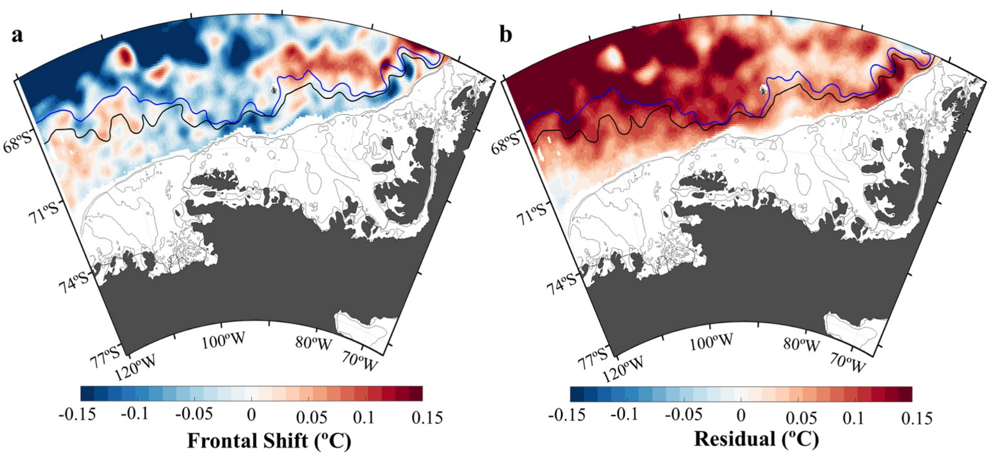

Figure 5. Influence of the interdecadal poleward displacement of the SACCF on the conservative temperature of the CDW layer. The total conservative temperature (Θ, °C) change between the 1990s and 2010s (Figure 1c) is decomposed into (a) the frontal displacement (°C) and (b) the residual term. Blue and black lines indicate the mean position of the Southern Antarctic Circumpolar Current Front (SACCF) during the 1990s and 2010s, respectively, based on GLORYS output. Thin gray contours represent the 500 m and 1,500 m isobaths from the R–Topo2 data set (Schaffer et al., 2016).

Instead, the dominant contribution to the observed warming arises from processes captured within the residual term (~0.09°C; ~90%; Figure 5b). In our decomposition of the conservative temperature of CDW, this term accounts for water mass property changes occurring along the core of CDW, independently of frontal displacement. Here, we interpret this dominant CDW warming as being indicative of enhanced lateral heat transport associated with Ross Gyre strengthening and increased meridional heat transport by cross-ACC exchanges. This contrasts with results from East Antarctica (80–60°E), where CDW warming has been more strongly linked to poleward displacement of the ACC fronts (Herraiz-Borreguero & Naveira Garabato, 2022; Yamazaki et al., 2021). This difference likely reflects distinct circulation regimes. Although regional gyres exist in East Antarctica (e.g., the Prydz Bay Gyre), their spatial extent and transport are more regionally confined compared to the basin-scale Ross Gyre (e.g., Yamazaki et al., 2020). Because lateral heat redistribution depends on both the strength and meridional extent of the circulation, smaller and more localized gyres might be expected to exert a more limited influence on large-scale isopycnal heat transfer. In contrast, the Ross Gyre spans a broader sector of the Pacific Southern Ocean and provides a more extensive pathway for lateral isopycnal heat transport toward West Antarctica (e.g., Nakayama et al., 2018). This interpretation is also consistent with the regional pattern of eddy kinetic energy change reported by Zhang et al. (2021), who found no coherent circumpolar increase in eddy kinetic energy but identified a significant increase downstream of the Campbell Plateau. Such regional enhancement may favor stronger cross-ACC isopycnal exchange in the Pacific sector, thereby contributing to lateral heat transport toward West Antarctica. This difference in circulation regimes may help explain why CDW variability in West Antarctica appears more influenced by Ross Gyre variability, whereas in East Antarctica it has been more closely linked to meridional displacements of ACC fronts.

Taken together, these results highlight the likely sensitivity of off-shelf CDW warming to wind-driven circulation changes. Because both SACCF displacement and isopycnal heat transport are linked to variability in the westerly winds, their relative contributions in future will depend on how continued wind intensification modulates gyre circulation, frontal structure, and mesoscale eddy activity. Climate projections indicate that sustained off-shelf warming in West Antarctica under intensified westerlies is probable, largely associated with Ross Gyre strengthening (Gómez-Valdivia et al., 2023). However, whether the fractional contribution of frontal displacement increases or remains secondary will require further scrutiny.

3.3. Long-Term Variability of CDW on the Continental Shelf

Having quantified the (likely wind-driven) warming of the off-shelf CDW layer, it is important to determine whether this enhanced heat reservoir can access the continental shelf. The presence of warmer off-shelf CDW does not necessarily lead to increased CDW intrusions, as highly dynamic shelf break processes and local thermodynamic forcing act as modulators (e.g., Couto et al., 2017; Dotto et al., 2019; Huguenin et al., 2024; Oelerich et al., 2022; Silvano et al., 2022; Webber et al., 2017). Although the mechanisms controlling CDW intrusions (e.g., local wind forcing and thermodynamic processes) are partly understood, their regional response to the atmospheric conditions of the 2010s remains unclear. In this section, we examine how interdecadal changes in shelf-break processes during the 2010s, primarily driven by ASL variability, modulated CDW intrusions and the regional expression of the off-shelf warming signal across the continental shelf of West Antarctica.

Despite overall warming of the off-shelf CDW around West Antarctica between the 1990s and the 2010s, the continental shelf exhibits pronounced spatial heterogeneity (Figure 1c). These spatial variations reflect the highly dynamic shelf break processes (e.g., local wind forcing at the shelf break) and thermodynamic processes within the continental shelf region (e.g., convection driven by surface heat loss and sea ice production), both of which are key to driving CDW thermohaline variability at the continental shelf (Azaneu et al., 2023; Dotto et al., 2019, 2020; Nakayama et al., 2018; Oelerich et al., 2022; Webber et al., 2017).

A similar regional dependence of CDW intrusions has also been documented in East Antarctica. There, the delivery of CDW onto the continental shelf is strongly modulated by local dynamical mechanisms, including isopycnal shoaling in regions such as Vincennes Bay (Ribeiro et al., 2025), variability in the Antarctic Slope Current, and wind-driven processes such as Ekman divergence poleward of the wind stress curl maximum (Greene et al., 2017; Kusahara et al., 2024; Nakayama et al., 2018). These studies emphasize that, although the large-scale circulation sets the off-shelf CDW heat reservoir around Antarctica, the actual intrusion of CDW onto the continental shelf is primarily controlled by regional oceanographic and atmospheric conditions.

Here, we found across the Amundsen Sea continental shelf, distinct hydrographic regimes emerge between the western and eastern basins, shaped by local bathymetry and the physical processes that regulate CDW intrusions at the shelf break. In the western basin, the CDW layer experienced a significant warming (area averaged ~0.10 ± 0.06°C; Figure 1c) between the decades of the 1990s and 2010s. These changes are likely linked to the presence of a deeper, more open trough (e.g., Cochran et al., 2020) that enables strong CDW inflow modulated by the Amundsen Sea undercurrent (e.g., Dotto et al., 2019). On interannual and decadal timescales, this undercurrent responds to zonal wind variability over the shelf break (Silvano et al., 2022). During the 2010s, a westward wind anomaly along the shelf break (Figure 6a), associated with a deeper and more intense ASL (Raphael et al., 2016; Figure 3d), steepened the Antarctic Slope Front by depressing isopycnals across the continental shelf (Figure 6c). This process strengthened the undercurrent, thereby facilitating greater CDW inflow (Figure 6c), which is consistent with the mechanism proposed by Silvano et al. (2022).

In contrast, the eastern Amundsen Sea basin experienced CDW cooling (area averaged ~ −0.11 ± 0.07°C; Figure 1c) between the 1990s and 2010s. Here, the troughs are shallower than the Dotson-Getz trough, vertically restricting CDW access. Consequently, the intrusion of warm water is critically dependent on the depth of the thermocline (e.g., Webber et al., 2017). We suggest that enhanced wintertime coastal-polynya activity in the eastern Amundsen Sea during the 2010s may have increased the production and retention of Winter Water observed in the following summer. The larger intermediate-depth reservoir of Winter Water strengthened stratification near the shelf break, deepened the summer thermocline, and depressed isopycnals, ultimately limiting the access of CDW-contained oceanic heat and contributing to regional cooling (e.g., O'Connor et al., 2025). An additional contributor to the observed cooling is the persistence of westward summertime wind anomalies along the continental shelf break (Figure 6a). These anomalies intensify surface-layer Ekman transport, reinforcing shelf-break convergence and promoting water mass accumulation in the upper ocean. This, combined with enhanced mixing between Winter Water and glacial meltwater (Huguenin et al., 2024; Webber et al., 2019), drives further isopycnal deepening and reduces the capacity of shelf-break processes to transport CDW onto the continental shelf via submarine troughs (Dotto et al., 2019; Dutrieux et al., 2014; Jacobs et al., 2011; Nakayama et al., 2013; Webber et al., 2017). This is evident in both Pine Island troughs (eastern and western troughs; Figures 6d and 6e).

Across the Bellingshausen Sea continental shelf, decadal differences in CDW layer properties also exhibit a pronounced contrast between eastern and western basins, likely reflecting the influence of the ASL on shelf break dynamics and thermodynamic processes. In the western basin, we observed cooling (area averaged ~ −0.10 ± 0.07°C; Figure 1c) associated with a westward wind anomaly at the shelf break (Figure 6a), consistent with the influence of a deeper and more intense ASL. This atmospheric state promotes enhanced on-shelf Ekman transport of cold surface waters, which reduces CDW inflow (e.g., Huguenin et al., 2024), as evidenced along the Belgica trough section (Figure 6f). Simultaneously, over the continental shelf, intensified northward and westward winds (Figures 6a and 6b) acted to reduce sea-ice concentration, favoring increased heat loss and convective processes, which combined lead to gradual cooling of continental shelf waters, as previously suggested by Oelerich et al. (2022).

Conversely, in the eastern Bellingshausen Sea basin, we observed CDW warming (area averaged ~0.17 ± 0.10°C; Figure 1c). Here, the influence of the ASL was weaker (Figure 3d), characterized by stronger northward wind anomalies and reduced westward wind anomalies (Figures 6a and 6b), conditions typically expected to restrict CDW intrusions due to enhanced off-shelf Ekman transport of cold surface waters (e.g., Huguenin et al., 2024). We therefore suggest that CDW warming observed in this region was most likely associated with enhanced CDW transfer by mesoscale eddy activity (Couto et al., 2017; Martinson & McKee, 2012; Moffat et al., 2009), likely facilitated by the closer proximity of the SACCF to the continental shelf break (Figure 1). Such dynamics are particularly evident in the Latady and Marguerite troughs (Figures 6g and 6h), where the enhanced CDW inflow can subsequently be advected westward, delivering heat to the Belgica trough (Figure 6f). These conditions appear to offset the local thermodynamic cooling processes also observed at the western Belligshausen Sea continental shelf basin. Such processes would typically cool the deeper water column, but here they are counteracted by the stronger inflow of warm CDW. Furthermore, the increased access of warmed CDW delivers heat to ice shelves and potentially intensifies basal melting, which would lead to enhanced local meltwater input in this region (e.g., Sheehan et al., 2023). This meltwater is likely subsequently transported by the Antarctic Coastal Current westward along the continental shelf, contributing freshwater to adjacent regions such as the western Bellingshausen and eastern Amundsen Seas (Schubert et al., 2021; Schulze Chretien et al., 2021; Thompson et al., 2020).

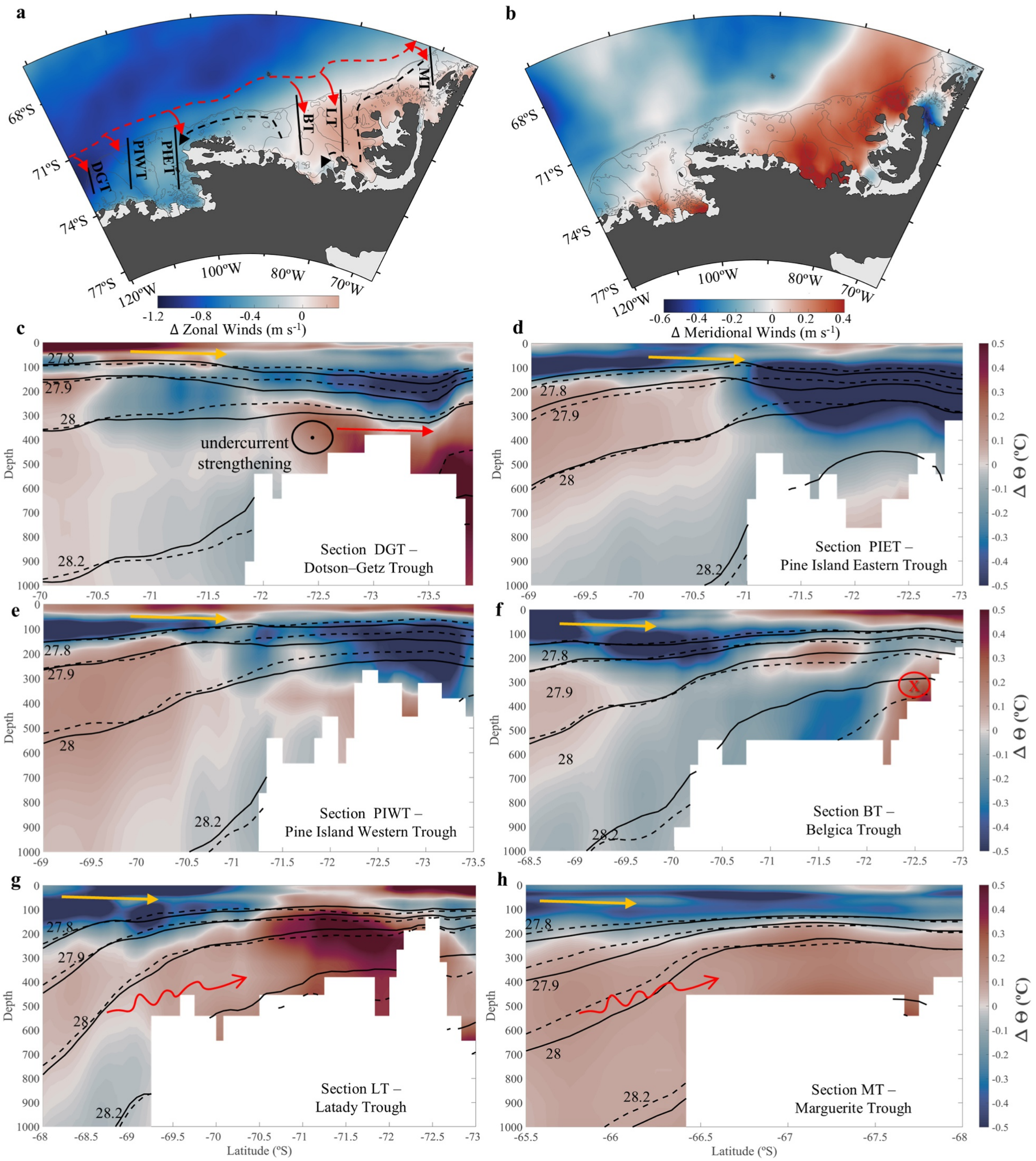

Figure 6. Wind-driven shift in the vertical structure of CDW intruding onto the West Antarctic continental shelf. (a, b) Interdecadal difference (2010s minus 1990s) in zonal and meridional wind speed anomalies (m s^{-1}) between two periods (i.e., 2010s minus 1990s), respectively. Thin gray contours represent the 500 m and 1,500 m isobaths from the R–Topo2 data set (Schaffer et al., 2016). The red arrows indicate CDW transfer across the Southern ACC front and its intrusions onto the continental shelf via troughs. (c–h) Decadal difference of Conservative Temperature (Θ, °C) in sections across the Dotson-Getz Trough (DGT), Pine Island Eastern Trough (PIET), Pine Island Western Trough (PIWT), Latady Trough (LT), Belgica Trough (BT), and Marguerite Trough (MT). The locations of these sections are shown as black lines in panel (a). The dashed and solid lines indicate the mean neutral density contours (27.8, 27.9, 28.0, and 28.2 kg m^{-3}) for the 1990s and 2010s, respectively. The red arrows highlight the inflow of CDW (including eddy-driven pathways indicated by curved arrows) onto the continental shelf, while yellow arrows denote surface water transports.

3.4. Key Limitations

Overall, hydrographic observations and the GLORYS output reanalysis show good qualitative agreement in representing the thermohaline structure of the off-shelf CDW (Figures S2 and S3 in Supporting Information S1). Quantitatively, differences between the two data sets reach up to ∼0.1°C in temperature and 0.15 g kg^{-1} in salinity (Figure S9 in Supporting Information S1). Despite these differences, the overall consistency indicates that GLORYS output captures the large-scale interdecadal variability of the off-shelf CDW reasonably well.

For clarity, we group the analysis into decades. Although the choice of temporal boundaries is somewhat arbitrary, the observed changes in CDW properties are consistent with a broader linear warming trend throughout the study period (Figure S8 in Supporting Information S1). The decadal averages, therefore, serve mainly as a practical way to illustrate longer-term variability rather than implying discrete shifts between time periods. We also note that the number of hydrographic profiles available varies between decades because observations in this region are sparse and irregular in time, with particularly limited coverage during the 1990s. This uneven sampling introduces some uncertainty when comparing decadal averages.

We highlighted that larger discrepancies appear over the continental shelf. Although GLORYS output reproduces the general pattern of interdecadal differences seen in hydrographic observations across much of the West Antarctic continental shelf (Figure 1), differences between observations and the reanalysis can reach ∼1.3°C in temperature and 0.3 g kg^{-1} in salinity (Figure S9 in Supporting Information S1). Several factors likely contribute to these differences. First, observational coverage over the continental shelf remains sparse and uneven through time, which increases uncertainty in decadal estimates. Second, the horizontal resolution of GLORYS output (∼8 km) does not fully resolve mesoscale dynamics in this region. Because the first baroclinic Rossby radius is about 4 km, resolving mesoscale eddies would require grid spacing closer to ∼1 km (Hattermann et al., 2014; Nøst et al., 2011; Thompson et al., 2014). These unresolved eddies play an important role in cross-shelf exchanges and may affect how CDW pathways toward the continental shelf are represented. Third, inaccuracies in bathymetry (particularly in the representation of submarine glacial troughs) that may lead to circulation pathways that differ from those in reality (Oelerich et al., 2022), even though these troughs strongly guide CDW intrusions onto the shelf. For these reasons, caution is needed when interpreting interdecadal variability of CDW properties on the continental shelf, including the influence of local wind forcing and on-shelf thermodynamic processes. Future studies that combine higher-resolution regional modeling with improved observational coverage will be important to resolve these processes better.

4. Conclusions and Outlook

Based on hydrographic measurements and reanalysis output, we show that an interdecadal warming and salinification of the off-shelf CDW layer in West Antarctica occurred between the 1990s and 2010s, most likely driven by wind-forced circulation changes. Specifically, the poleward shift and intensification of the westerly winds strengthened the Ross Gyre, predictably enhancing lateral heat transport along isopycnals in the SACCF region and cross-ACC isopycnal exchange. These advective processes account for approximately 90% of the observed CDW warming. Although we also identified an interdecadal poleward displacement of the SACCF around West Antarctica, our results indicate that this frontal shift contributed only about 10% and therefore played a secondary role.

While we observe an increase in the contribution of warmer, saltier CDW along the off–shelf region, GLORYS outputs suggest that intrusion of this water onto the adjacent continental shelf may have been inhibited in some areas (i.e., eastern Amundsen and western Bellingshausen Seas) due to a westward wind anomaly there, potentially linked to a deepened and intensified ASL. In contrast, due to the specific conditions of each region (i.e., the extent of the influence of the Amundsen undercurrent and of eddy activity near the SACCF), this warmed CDW can penetrate onto the continental shelf of the western Amundsen and eastern Bellingshausen Seas, leading to a warming and salinification of those areas. Additionally, thermodynamic processes associated with the sea-ice production and surface heat loss on the continental shelf might also have contributed to changes in CDW layer properties. Thus, our results evidence the importance of the localized processes over the shelf break and continental shelf (e.g., local wind forcing and thermodynamic processes) in regulating the extent to which CDW changes offshore may affect the shelf regions. These findings highlight the complex interplay between large-scale atmospheric forcing, ACC frontal dynamics, and regional oceanographic processes in shaping the evolution of CDW properties around West Antarctica.

Ongoing atmospheric trends are toward an intensified and poleward displacement of the Southern Hemisphere westerlies (e.g., Marshall, 2003), which are expected to modulate the large-scale ocean circulation (e.g., the Ross Gyre strength and eastward expansion; Dotto et al., 2018). As documented here, such changes can lead to off-shelf CDW warming, which could, in the long-term, enhance the intrusion of this warmer water onto the continental shelf in some regions of West Antarctica and, in turn, compromise the stability of the ice sheet in those areas, with implications for global sea-level rise. Therefore, ongoing monitoring and the use of high-resolution ocean-ice models are vital to better understand the mechanistic linkages between large-scale climatic changes over the ACC and Ross Gyre, variations in the cross-shelf transfer of CDW, and coastal ocean-ice interactions in this climatically sensitive region.

Acknowledgments

This study is part of the Brazilian High Latitude Oceanography Group (GOAL) activities within the Brazilian Antarctic Program (PROANTAR). GOAL has been funded by and/or has received logistical support from the Brazilian Ministry of the Environment (MMA); the Brazilian Ministry of Science, Technology, and Innovation (MCTI); the Council for Research and Scientific Development of Brazil (CNPq); the National Institute of Science and Technology of the Cryosphere (INCT CRIOSFERA; CNPq Grant. 573720/2008-8, 465680/2014-3 and 408461/2024-1); and the Research Support Foundation of the State of Rio Grande do Sul (FAPERGS Grant 17/2551-000518-0). This study was conducted within the activities of the GOAL projects (CNPq Grant 440865/2023-9) and CARBON Team activities (www.carbonteam.furg.br). Financial support was also received from Coordination for the Improvement of Higher Education Personnel (CAPES) through the project CAPES "Ciências do Mar" (Grant 23038.001421/2014-30). CAPES also provided free access to many relevant journals through the portal "Periódicos CAPES" and the activities of the Graduate Program in Oceanology. This study is from the TARSAN project, a component of the International Thwaites Glacier Collaboration (ITGC). Support from National Science Foundation (NSF: Grant 1929991) and Natural Environment Research Council (NERC: Grant NE/S006419/1). Logistics provided by NSF-U.S. Antarctic Program and NERC-British Antarctic Survey. ITGC Contribution No. ITGC-159. Brendon Y. Damini acknowledges financial support from CAPES PhD. Scholarship Grant 88887.719848/2022-00 and 88881.982653/2024-01. Tiago S. Dotto was supported by the NERC National Capability programme AtlantiS (NE/Y005589/1). Karen J. Heywood and Rob A. Hall were supported by the Natural Environment Research Council (NERC) Grant NE/P021395/1, NE/S006419/1 and NE/W007045/1. Alberto C. Naveira Garabato acknowledges UK Research and Innovation guarantee funding for a European Research Council Advanced Grant (EP/X025136/1). Rodrigo Kerr and Mauricio M. Mata are granted researcher fellowships from CNPq Grant 309978/2021-1 and 312569/2021-1. The Article Processing Charge for the publication of this research was funded by the Coordenação de Aperfeiçoamento de Pessoal de Nível Superior - Brasil (CAPES) (ROR identifier: 00x0ma614).

Conflict of Interest

The authors declare no conflicts of interest relevant to this study.

Availability Statement

Hydrographic seawater temperature and salinity data (1990–2020) were obtained from the following publicly available repositories: World Ocean Database 2023 (WOD23; https://www.ncei.noaa.gov/products/world-ocean-database; Mishonov et al., 2024); Thwaites-Amundsen Regional Survey and Network (TARSAN; https://www.bodc.ac.uk/data/bodc_database/nodb/project/54319/); Argo float data (Argo, 2000; https://argo.ucsd.edu); CLIVAR and Carbon Hydrographic Data Office (CCHDO; https://cchdo.ucsd.edu/); and Marine Mammals Exploring the Ocean Pole to Pole (MEOP; https://www.meop.net/; Roquet et al., 2011). Ocean reanalysis temperature and salinity fields were obtained from the GLORYS12v1 global ocean reanalysis (https://doi.org/10.48670/moi-00021; Fernandez & Lellouche, 2021). Monthly wind stress and sea level pressure fields were obtained from the ERA5 reanalysis (https://doi.org/10.24381/cds.f17050d7; Hersbach et al., 2020). ADT fields were obtained from the Copernicus Marine Service (https://doi.org/10.48670/moi-00148). The Antarctic Circumpolar Current front positions are based on Orsi et al. (1995) and are available from the Australian Antarctic Data Centre (https://data.aad.gov.au/metadata/records/antarctic_circumpolar_current_fronts/; Orsi & Harris, 2019). Bathymetric data were obtained from R–Topo2 data set (https://doi.org/10.1594/PANGAEA.85684; Schaffer et al., 2016).

References

Argo. (2000). *Argo float data and metadata from Global Data Assembly Centre (Argo GDAC)*. SEANOE. https://doi.org/10.17882/42182

Auger, M., Morrow, R., Kestenare, E., Sallée, J. B., & Cowley, R. (2021). Southern Ocean in-situ temperature trends over 25 years emerge from interannual variability. *Nature Communications*, *12*(1), 514. https://doi.org/10.1038/s41467-020-20781-1

Azaneu, M., Webber, B., Heywood, K. J., Assmann, K. M., Dotto, T. S., & Abrahamsen, E. P. (2023). Influence of Shelf break processes on the transport of warm waters onto the Eastern Amundsen Sea Continental Shelf. *Journal of Geophysical Research: Oceans*, *128*(5), e2022JC019535. https://doi.org/10.1029/2022JC019535

Böning, C. W., Dispert, A., Visbeck, M., Rintoul, S. R., & Schwarzkopf, F. U. (2008). The response of the Antarctic Circumpolar Current to recent climate change. *Nature Geoscience*, *1*(12), 864–869. https://doi.org/10.1038/ngeo362

Castagno, P., Falco, P., Dinniman, M. S., Spezie, G., & Budillon, G. (2017). Temporal variability of the Circumpolar Deep Water inflow onto the Ross Sea continental shelf. *Journal of Marine Systems*, *166*, 37–49. https://doi.org/10.1016/j.jmarsys.2016.07.007

Chapman, C. C. (2014). Southern Ocean jets and how to find them: Improving and comparing common jet detection methods. *Journal of Geophysical Research: Oceans*, *119*(7), 4318–4339. https://doi.org/10.1002/2014JC009810

Chapman, C. C., Lea, M. A., Meyer, A., Sallée, J. B., & Hindell, M. (2020). Defining Southern Ocean fronts and their influence on biological and physical processes in a changing climate. *Nature Climate Change*, *10*(3), 209–219. https://doi.org/10.1038/s41558-020-0705-4

Clem, K. R., & Fogt, R. L. (2015). South Pacific circulation changes and their connection to the tropics and regional Antarctic warming in austral spring, 1979-2012. *Journal of Geophysical Research*, *120*(7), 2773–2792. https://doi.org/10.1002/2014JD022940

Cochran, J. R., Tinto, K. J., & Bell, R. E. (2020). Detailed bathymetry of the Continental shelf beneath the Getz Ice Shelf, West Antarctica. *Journal of Geophysical Research: Earth Surface*, *125*(10), e2019JF005493. https://doi.org/10.1029/2019JF005493

Couto, N., Martinson, D. G., Kohut, J., & Schofield, O. (2017). Distribution of upper circumpolar deep water on the warming continental shelf of the West Antarctic Peninsula. *Journal of Geophysical Research: Oceans*, *122*(7), 5306–5315. https://doi.org/10.1002/2017JC012840

Cowley, R., Killick, R. E., Boyer, T., Gouretski, V., Reseghetti, F., Kizu, S., et al. (2021). International quality-controlled ocean database (IQuOD) v0.1: The temperature uncertainty specification. *Frontiers in Marine Science*, *8*, 689695. https://doi.org/10.3389/fmars.2021.689695

Damini, B. Y., Brum, A. L., Hall, R. A., Dotto, T. S., Azevedo, J. L. L., Heywood, K. J., et al. (2025). Summer circulation and water masses transport in Bransfield Strait, Antarctica: An evaluation of their response to combined effects of Southern Annular Mode and El Niño–Southern Oscillation. *Deep Sea Research Part I: Oceanographic Research Papers*, *222*, 104516. https://doi.org/10.1016/J.DSR.2025.104516

Dong, X., Wang, Y., Shugui, H. O. U., Ding, M., Baoling, Y. I. N., & Zhang, Y. (2020). Robustness of the recent global atmospheric reanalyses for antarctic near-surface wind speed climatology. *Journal of Climate*, *33*(10), 4027–4043. https://doi.org/10.1175/JCLI-D-19-0648.1

Dotto, T. S., Garabato, A. C. N., Bacon, S., Holland, P. R., Kimura, S., Firing, Y. L., et al. (2019). Wind-driven processes controlling oceanic heat delivery to the Amundsen Sea, Antarctica. *Journal of Physical Oceanography*, *49*(11), 2829–2849. https://doi.org/10.1175/JPO-D-19-0064.1

Dotto, T. S., Naveira Garabato, A., Bacon, S., Tsamados, M., Holland, P. R., Hooley, J., et al. (2018). Variability of the ross gyre, Southern Ocean: Drivers and responses revealed by satellite altimetry. *Geophysical Research Letters*, *45*(12), 6195–6204. https://doi.org/10.1029/2018GL078607

Dotto, T. S., Naveira Garabato, A. C., Wåhlin, A. K., Bacon, S., Holland, P. R., Kimura, S., et al. (2020). Control of the oceanic heat content of the Getz-Dotson Trough, Antarctica, by the Amundsen Sea Low. *Journal of Geophysical Research: Oceans*, *125*(8), e2020JC016113. https://doi.org/10.1029/2020JC016113

Dufour, C. O., Griffies, S. M., de Souza, G. F., Frenger, I., Morrison, A. K., Palter, J. B., et al. (2015). Role of mesoscale eddies in cross-frontal transport of heat and biogeochemical tracers in the Southern Ocean. *Journal of Physical Oceanography*, *45*(12), 3057–3081. https://doi.org/10.1175/JPO-D-14-0240.1

Dutrieux, P., Stewart, C., Jenkins, A., Nicholls, K. W., Corr, H. F. J., Rignot, E., & Steffen, K. (2014). Basal terraces on melting ice shelves. *Geophysical Research Letters*, *41*(15), 5506–5513. https://doi.org/10.1002/2014GL060618

Fernandez, E., & Lellouche, J. M. (2021). Product user manual for Global Ocean Reanalysis Products GLOBAL_REANALYSIS_PHY_001_030. CMEMS-GLO-QUID-001-030 (pp. 1–21).

Ferrari, R., & Nikurashin, M. (2010). Suppression of eddy diffusivity across jets in the Southern Ocean. *Journal of Physical Oceanography*, *40*(7), 1501–1519. https://doi.org/10.1175/2010JPO4278.1

Frederikse, T., Landerer, F., Caron, L., Adhikari, S., Parkes, D., Humphrey, V. W., et al. (2020). The causes of sea-level rise since 1900. *Nature 2020*, *584*(7821), 393–397. https://doi.org/10.1038/s41586-020-2591-3

Gille, S. T. (2002). Warming of the Southern Ocean since the 1950s. *Science*, *295*(5558), 1275–1277. https://doi.org/10.1126/SCIENCE.1065863

Gille, S. T. (2008). Decadal-scale temperature trends in the Southern Hemisphere ocean. *Journal of Climate*, *21*(18), 4749–4765. https://doi.org/10.1175/2008JCLI2131.1

Gille, S. T. (2014). Meridional displacement of the Antarctic Circumpolar Current. *Philosophical Transactions of the Royal Society A: Mathematical, Physical and Engineering Sciences*, *372*(2019), 20130273. https://doi.org/10.1098/RSTA.2013.0273

Gómez-Valdivia, F., Holland, P. R., Siahaan, A., Dutrieux, P., & Young, E. (2023). Projected West Antarctic ocean warming caused by an expansion of the Ross Gyre. *Geophysical Research Letters*, *50*(6), e2023GL102978. https://doi.org/10.1029/2023gl102978

Goyal, R., Sen Gupta, A., Jucker, M., & England, M. H. (2021). Historical and projected changes in the Southern hemisphere surface westerlies. *Geophysical Research Letters*, *48*(4), e2020GL090849. https://doi.org/10.1029/2020GL090849

Greene, C. A., Blankenship, D. D., Gwyther, D. E., Silvano, A., & van Wijk, E. (2017). Wind causes Totten Ice Shelf melt and acceleration. *Science Advances*, *3*(11), e1701681. https://doi.org/10.1126/sciadv.1701681

Hattermann, T., Smedsrud, L. H., Nøst, O. A., Lilly, J. M., & Galton-Fenzi, B. K. (2014). Eddy resolving simulations of the Fimbul Ice Shelf cavity circulation: Basal melting and exchange with open ocean. *Ocean Modelling*, *82*, 28–44. https://doi.org/10.1016/j.ocemod.2014.07.004

Herraiz-Borreguero, L., & Naveira Garabato, A. C. (2022). Poleward shift of circumpolar deep water threatens the East Antarctic Ice sheet. *Nature Climate Change 2022*, *12*(8), 728–734. https://doi.org/10.1038/s41558-022-01424-3

Hersbach, H., Bell, B., Berrisford, P., Hirahara, S., Horányi, A., Muñoz-Sabater, J., et al. (2020). The ERA5 global reanalysis. *Quarterly Journal of the Royal Meteorological Society*, *146*(730), 1999–2049. https://doi.org/10.1002/QJ.3803

Hosking, J. S., Orr, A., Marshall, G. J., Turner, J., & Phillips, T. (2013). The influence of the Amundsen–Bellingshausen Seas low on the climate of West Antarctica and its representation in coupled climate model simulations. *Journal of Climate*, *26*(17), 6633–6648. https://doi.org/10.1175/JCLI-D-12-00813.1

Huguenin, M. F., Holmes, R. M., Spence, P., & England, M. H. (2024). Subsurface warming of the West Antarctic continental shelf linked to El Niño-Southern Oscillation. *Geophysical Research Letters*, *51*(7), e2023GL104518. https://doi.org/10.1029/2023GL104518

Jacobs, S. S., Jenkins, A., Giulivi, C. F., & Dutrieux, P. (2011). Stronger ocean circulation and increased melting under Pine Island Glacier ice shelf. *Nature Geoscience*, *4*(8), 519–523. https://doi.org/10.1038/ngeo1188

Jean-Michel, L., Eric, G., Romain, B. B., Gilles, G., Angélique, M., Marie, D., et al. (2021). The copernicus Global 1/12° Oceanic and Sea ice GLORYS12 reanalysis. *Frontiers in Earth Science*, *9*, 698876. https://doi.org/10.3389/feart.2021.698876

Kim, Y. S., & Orsi, A. H. (2014). On the variability of Antarctic circumpolar current fronts inferred from 1992–2011 altimetry. *Journal of Physical Oceanography*, *44*(12), 3054–3071. https://doi.org/10.1175/JPO-D-13-0217.1

Kusahara, K., Hirano, D., Fujii, M., Fraser, A. D., Tamura, T., Mizobata, K., et al. (2024). Modeling seasonal-to-decadal ocean–cryosphere interactions along the Sabrina Coast, East Antarctica. *The Cryosphere*, *18*(1), 43–73. https://doi.org/10.5194/tc-18-43-2024

Marshall, G. J. (2003). Trends in the Southern Annular Mode from observations and reanalyses. *Journal of Climate*, *16*(24), 4134–4143. https://doi.org/10.1175/1520-0442(2003)016<4134:TITSAM>2.0.CO;2

Marshall, J., & Speer, K. (2012). Closure of the meridional overturning circulation through Southern Ocean upwelling. *Nature Geoscience*, *5*(3), 171–180. https://doi.org/10.1038/ngeo1391

Martinson, D. G., & McKee, D. C. (2012). Transport of warm upper circumpolar deep water onto the Western Antarctic Peninsula Continental Shelf. *Ocean Science*, *8*(4), 433–442. https://doi.org/10.5194/OS-8-433-2012

McDougall, T. J., & Barker, P. M. (2011). Getting started with TEOS-10 and the Gibbs Seawater (GSW). *Scor/Iapso Wg127*, *28*. Retrieved from http://www.teos-10.org/pubs/gsw/v3_04/pdf/Getting_Started.pdf

Mckee, D. C., Martinson, D. G., & Schofield, O. (2019). Origin and attenuation of mesoscale structure in circumpolar deep water intrusions to an Antarctic Shelf. *Journal of Physical Oceanography*, *49*(5), 1293–1318. https://doi.org/10.1175/JPO-D-18-0133.1

Meijers, A. J. S., Bindoff, N. L., & Rintoul, S. R. (2011). Frontal movements and property fluxes: Contributions to heat and freshwater trends in the Southern Ocean. *Journal of Geophysical Research*, *116*(8), 8024. https://doi.org/10.1029/2010JC006832

Meredith, M. P. (2016). Understanding the structure of changes in the Southern Ocean eddy field. *Geophysical Research Letters*, *43*(11), 5829–5832. https://doi.org/10.1002/2016GL069677

Mishonov, A. V., Boyer, T. P., Baranova, O. K., Bouchard, C. N., Cross, S., Garcia, H. E., et al. (2024). World Ocean Database 2023. C. Bouchard (Technical Ed.), NOAA Atlas NESDIS (Vol. 97, p. 206). https://doi.org/10.25923/z885-h264

Mizobata, K., Hirano, D., Kusahara, K., Aoki, S., Inoue, J., Takao, S., & Makabe, R. (2025). Ocean response along the east Antarctic coastal margin to the southern annular mode. *Geophysical Research Letters*, *52*(6), e2024GL112914. https://doi.org/10.1029/2024gl112914

Moffat, C., Owens, B., & Beardsley, R. C. (2009). On the characteristics of Circumpolar Deep Water intrusions to the west Antarctic Peninsula Continental Shelf. *Journal of Geophysical Research*, *114*(C5). https://doi.org/10.1029/2008JC004955

Nakayama, Y., Menemenlis, D., Zhang, H., Schodlok, M., & Rignot, E. (2018). Origin of Circumpolar Deep Water intruding onto the Amundsen and Bellingshausen Sea continental shelves. *Nature Communications*, *9*(1), 3403. https://doi.org/10.1038/s41467-018-05813-1

Nakayama, Y., Schröder, M., & Hellmer, H. H. (2013). From circumpolar deep water to the glacial meltwater plume on the eastern Amundsen Shelf. *Deep Sea Research Part I: Oceanographic Research Papers*, *77*, 50–62. https://doi.org/10.1016/J.DSR.2013.04.001

Nøst, O. A., Biuw, M., Tverberg, V., Lydersen, C., Hattermann, T., Zhou, Q., et al. (2011). Eddy overturning of the Antarctic slope front controls glacial melting in the Eastern Weddell Sea. *J. Geophys. Res.Ocean*, *116*(C11). https://doi.org/10.1029/2011JC006965

O'Connor, G. K., Nakayama, Y., Steig, E. J., Armour, K. C., Thompson, L. A., Hyogo, S., et al. (2025). Enhanced West Antarctic ice loss triggered by polynya response to meridional winds. *Nature Geoscience*, *18*(9), 840–847. https://doi.org/10.1038/s41561-025-01757-6

Oelerich, R., Heywood, K. J., Damerell, G. M., & Thompson, A. F. (2022). Wind-Induced variability of warm water on the Southern Bellingshausen Sea Continental Shelf. *Journal of Geophysical Research: Oceans*, *127*(11), e2022JC018636. https://doi.org/10.1029/2022JC018636

Orsi, A. H., & Harris, U. (2019). *Fronts of the Antarctic Circumpolar Current - GIS data, Ver. 1*. Australian Antarctic Data Centre. Retrieved from https://data.aad.gov.au/metadata/antarctic_circumpolar_current_fronts

Orsi, A. H., Whitworth, T., & Nowlin, W. D. (1995). On the meridional extent and fronts of the Antarctic Circumpolar Current. *Deep-Sea Research Part I*, *42*(5), 641–673. https://doi.org/10.1016/0967-0637(95)00021-W

Park, Y. H., Park, T., Kim, T. W., Lee, S. H., Hong, C. S., Lee, J. H., et al. (2019). Observations of the Antarctic Circumpolar Current over the Udintsev Fracture Zone, the narrowest Choke point in the Southern Ocean. *Journal of Geophysical Research: Oceans*, *124*(7), 4511–4528. https://doi.org/10.1029/2019JC015024

Prend, C. J., MacGilchrist, G. A., Manucharyan, G. E., Pang, R. Q., Moorman, R., Thompson, A. F., et al. (2024). Ross Gyre variability modulates oceanic heat supply toward the West Antarctic continental shelf. *Communications Earth & Environment*, *5*(1), 47. https://doi.org/10.1038/s43247-024-01207-y

Raphael, M. N., Marshall, G. J., Turner, J., Fogt, R. L., Schneider, D., Dixon, D. A., et al. (2016). The Amundsen Sea low: Variability, change, and impact on antarctic climate. *Bulletin of the American Meteorological Society*, *97*(1), 111–121. https://doi.org/10.1175/BAMS-D-14-00018.1

Ribeiro, N., Herraiz-Borreguero, L., Rintoul, S. R., Williams, G., McMahon, C. R., Hindell, M., & Guinet, C. (2023). Oceanic regime shift to a warmer continental shelf adjacent to the Shackleton Ice Shelf, East Antarctica. *Journal of Geophysical Research: Oceans*, *128*(11), e2023JC019882. https://doi.org/10.1029/2023JC019882

Ribeiro, N., Morrison, A. K., Rintoul, S. R., Bindoff, N. L., Herraiz-Borreguero, L., & Williams, G. (2025). Wind-driven variability of modified Circumpolar Deep Water intrusions into Vincennes Bay, East Antarctica. *Journal of Geophysical Research: Oceans*, *130*(11), e2025JC022843. https://doi.org/10.1029/2025JC022843

Rignot, E., Mouginot, J., Scheuchl, B., Van Den Broeke, M., Van Wessem, M. J., & Morlighem, M. (2019). Four decades of Antarctic ice sheet mass balance from 1979–2017. *Proceedings of the National Academy of Sciences of the United States of America*, *116*(4), 1095–1103. https://doi.org/10.1073/pnas.1812883116

Riser, S. C., Ren, L., & Wong, A. (2015). Salinity in Argo: A modern view of a changing ocean. *Oceanography*, *21*(1), 56–67. https://doi.org/10.5670/oceanog.2008.67

Roquet, F., Charrassin, J.-B., Marchand, S., Boehme, L., Fedak, M., Reverdin, G., & Guinet, C. (2011). Delayed-mode calibration of hydrographic data obtained from animal-borne satellite relay data loggers. *Journal of Atmospheric and Oceanic Technology*, *28*(6), 787–801. https://doi.org/10.1175/2010JTECHO801.1

Sallée, J. B. (2018). Southern ocean warming. *Oceanography*, *31*(2 Special Issue), 52–62. https://doi.org/10.5670/OCEANOG.2018.215

Schaffer, J., Timmermann, R., Arndt, J. E., Kristensen, S. S., Mayer, C., Morlighem, M., & Steinhage, D. (2016). A global, high-resolution data set of ice sheet topography, cavity geometry, and ocean bathymetry. *Earth System Science Data*, *8*(2), 543–557. https://doi.org/10.5194/essd-8-543-2016

Schiavon, G., Gille, S. T., & Oliveira, F. S. C. (2025). Response of Antarctic Circumpolar Current Jets to Southern Hemisphere Westerly Shifts during the 21st century. *Journal of Geophysical Research: Oceans*, *130*(12), e2025JC022897. https://doi.org/10.1029/2025JC022897

Schmidtko, S., Heywood, K. J., Thompson, A. F., & Aoki, S. (2014). Multidecadal warming of Antarctic waters. *Science*, *346*(6214), 1227–1231. https://doi.org/10.1126/SCIENCE.1256117

Schubert, R., Thompson, A. F., Speer, K., Schulze Chretien, L., & Bebieva, Y. (2021). The Antarctic coastal current in the Bellingshausen Sea. *The Cryosphere*, *15*(9), 4179–4199. https://doi.org/10.5194/TC-15-4179-2021

Schulze Chretien, L. M., Thompson, A. F., Flexas, M. M., Speer, K., Swaim, N., Oelerich, R., et al. (2021). The shelf circulation of the Bellingshausen Sea. *Journal of Geophysical Research: Oceans*, *126*(5), e2020JC016871. https://doi.org/10.1029/2020JC016871

Sheehan, P. M. F., Heywood, K. J., Thompson, A. F., Flexas, M. M., & Schodlok, M. P. (2023). Sources and pathways of glacial meltwater in the Bellingshausen Sea, Antarctica. *Geophysical Research Letters*, *50*(14), e2023GL102785. https://doi.org/10.1029/2023GL102785

Siegelman, L., Roquet, F., Mensah, V., Rivière, P., Pauthenet, E., Picard, B., & Guinet, C. (2019). Correction and accuracy of High- and low-resolution CTD data from animal-borne instruments. *Journal of Atmospheric and Oceanic Technology*, *36*(5), 745–760. https://doi.org/10.1175/JTECH-D-18-0170.1

Silvano, A., Holland, P. R., Naughten, K. A., Dragomir, O., Dutrieux, P., Jenkins, A., et al. (2022). Baroclinic Ocean response to climate forcing regulates decadal variability of ice-shelf melting in the Amundsen Sea. *Geophysical Research Letters*, *49*(24), e2022GL100646. https://doi.org/10.1029/2022GL100646

Sokolov, S., & Rintoul, S. R. (2009a). Circumpolar structure and distribution of the Antarctic circumpolar current fronts: 1. Mean 98 circumpolar paths. *Journal of Geophysical Research*, *114*(11), 11018. https://doi.org/10.1029/2008JC005108

Sokolov, S., & Rintoul, S. R. (2009b). Circumpolar structure and distribution of the Antarctic circumpolar Current fronts: 2. Variability and relationship to sea surface height. *Journal of Geophysical Research*, *114*(C11). https://doi.org/10.1029/2008JC005248

Thompson, A. F., Heywood, K. J., Schmidtko, S., & Stewart, A. L. (2014). Eddy transport as a key component of the Antarctic overturning circulation. *Nature Geoscience*, *7*(12), 171–180. https://doi.org/10.1038/NGEO2289

Thompson, A. F., & Naveira Garabato, A. C. (2014). Equilibration of the Antarctic Circumpolar Current by standing meanders. *Journal of Physical Oceanography*, *44*(7), 1811–1828. https://doi.org/10.1175/JPO-D-13-0163.1

Thompson, A. F., Speer, K. G., & Schulze Chretien, L. M. (2020). Genesis of the Antarctic slope current in West Antarctica. *Geophysical Research Letters*, *47*(16), e2020GL087802. https://doi.org/10.1029/2020GL087802

Turner, J., Orr, A., Gudmundsson, G. H., Jenkins, A., Bingham, R. G., Hillenbrand, C. D., & Bracegirdle, T. J. (2017). Atmosphere-ocean-ice interactions in the Amundsen Sea Embayment, West Antarctica. *Reviews of Geophysics*, *55*(1), 235–276. https://doi.org/10.1002/2016RG000532

Veny, M., Aguiar-González, B., Marrero-Díaz, Á., Pereira-Vázquez, T., & Rodríguez-Santana, Á. (2024). Biophysical coupling of seasonal chlorophyll-a bloom variations and phytoplankton assemblages across the Peninsula Front in the Bransfield Strait. *Ocean Science*, *20*(2), 389–415. https://doi.org/10.5194/OS-20-389-2024

Webber, B. G. M., Heywood, K. J., Stevens, D. P., Dutrieux, P., Abrahamsen, E. P., Jenkins, A., et al. (2017). Mechanisms driving variability in the ocean forcing of Pine Island Glacier. *Nature Communications*, *8*(1), 14507. https://doi.org/10.1038/ncomms14507

Webber, B. G. M., Heywood, K. J., Stevens, D. P., & Assmann, K. M. (2019). The impact of overturning and horizontal circulation in pine island trough on ice shelf melt in the eastern Amundsen Sea. *Journal of Physical Oceanography*, *49*(1), 63–83. https://doi.org/10.1175/JPO-D-17-0213.1

Yamazaki, K., Aoki, S., Katsumata, K., Hirano, D., & Nakayama, Y. (2021). Multidecadal poleward shift of the southern boundary of the Antarctic Circumpolar Current off East Antarctica. *Science Advances*, *7*(24), 8755–8766. https://doi.org/10.1126/sciadv.abf8755

Yamazaki, K., Aoki, S., & Mizobata, K. (2023). Diffusion of circumpolar deep water towards Antarctica. *Journal of Geophysical Research: Oceans*, *128*(2), e2022JC019422. https://doi.org/10.1029/2022JC019422

Yamazaki, K., Aoki, S., Shimada, K., Kobayashi, T., & Kitade, Y. (2020). Structure of the subpolar gyre in the Australian-Antarctic basin derived from Argo floats. *Journal of Geophysical Research: Oceans*, *125*(8), e2019JC015406. https://doi.org/10.1029/2019JC015406

Yamazaki, K., Katsumata, K., Hirano, D., Nomura, D., Sasaki, H., Murase, H., & Aoki, S. (2024). Revisiting circulation and water masses over the East Antarctic margin (80–150°E). *Progress in Oceanography*, *225*, 103285. https://doi.org/10.1016/j.pocean.2024.103285

Zhang, Y., Chambers, D., & Liang, X. (2021). Regional trends in Southern Ocean Eddy kinetic energy. *Journal of Geophysical Research: Oceans*, *126*(6), e2020JC016973. https://doi.org/10.1029/2020JC016973

Zu, Y., Gao, L., Guo, G., & Fang, Y. (2022). Changes of Circumpolar Deep Water between 2006 and 2020 in the south-west Indian Ocean, East Antarctica. *Deep Sea Research Part II: Topical Studies in Oceanography*, *197*, 105043. https://doi.org/10.1016/J.DSR2.2022.105043